Phase diagram of branched polymer collapse

Malte Henkel[1,2]* and Flavio Seno[3]
[1]Theoretical Physics, Department of Physics, University of Oxford, 1 Keble Road, Oxford OX1 3NP, England
[2]Laboratoire de Physique du Solide, CNRS URA No. 155, Université Henri Poincaré Nancy I, Boîte Postale 239, F-54506 Vandoeuvre lès Nancy Cedex, France
[3]Dipartimento di Fisica, Istituto Nazionale di Fisica della Materia, Università di Padova, Via Marzolo 8, I-35100 Padova, Italy
(Received 13 November 1995)

The phase diagram of the collapse of a two-dimensional infinite branched polymer interacting with the solvent and with itself through contact interactions is studied from the $q \to 1$ limit of an extension of the q-state Potts model. Exact solution on the Bethe lattice and Migdal-Kadanoff renormalization group calculations shows that there is a line of θ transitions from the extended to a single compact phase. The θ line, governed by three different fixed points, consists of two lines of extended-compact transitions which are in different universality classes and meet in a multicritical point. On the other hand, directed branched polymers are shown to be completely determined by the strongly embedded case and there is a single θ transition which is in the directed percolation universality class.

PACS number(s): 05.70.Jk, 64.60.Ak, 36.20.Ey, 64.60.Fr

I. INTRODUCTION

A long-standing problem in the theory of polymer molecules in solution is the effect of intramolecular forces on the shape and size of an isolated polymer. The intramolecular forces are usually assumed [1] to be of van der Waals type, consisting of strong, short-range repulsive and weak, long-range attractive interactions. Depending on temperature or solvent composition, the macromolecule forms either extended structures or collapses into a dense globule [2]. The transition between these two states, which is called θ transition, has attracted a great deal of attention, both theoretically [3–13] and experimentally, partly because of its connection with protein folding [14–16].

For the bidimensional *linear* polymers many theoretical tools, such as conformal invariance [17,18] and Coulomb gas [19] methods, can be successfully employed and considerable progress has been made in understanding the nature and the critical exponents at the collapse transition [20,21].

In contrast, much less is known about *branched* polymers. In lattice statistical mechanics they are described by lattice animals, graphs of connected occupied sites on a lattice. Some examples are shown in Fig. 1. *Contact* interactions are introduced between nearest neighbor sites which are not immediately linked by a bond and *solvent* interactions are introduced between an occupied site and any nearest neighbor empty sites. In d dimensions lattice animal exponents are related to the exponents of the Lee-Yang edge singularity of the Ising model in $d-2$ dimensions [22]. However, this elegant theoretical approach can give only the bulk entropic exponent for the extended phase. Moreover, branched polymers in two dimensions are in general not conformally invariant [23]. This model can be reformulated as the $q \to 1$ limit of an appropriate q-state Potts model [24,25]. However, this formulation has not given any exact results [26] but only allowed the conjecture that lattice animals could present two distinct branches of θ behavior, separated by a percolation critical point [9–11].

While there is little exact or analytical information available for this problem, a large amount of numerical work has been done using Monte Carlo [27–29], exact enumeration [30,8,9], and transfer matrix [31,11] methods. The results of these analyses are controversial, however, and it is this which triggered the work to be described here.

In order to describe the purposes and the goals of this paper let us first introduce some notation.

Let n, b, s, and k denote the number of sites, bonds, solvent interactions, and contact interactions of the lattice animal. We are working on a square lattice with coordination number $\gamma=4$. Then the relation $\gamma n = 2b + 2k + s$ implies that three of the four variables are needed to specify the problem completely. (In two dimensions, this is valid for $\gamma \leqslant 4$.) The statistical mechanics of the model is most conveniently described by a generating function. This has recently been de-

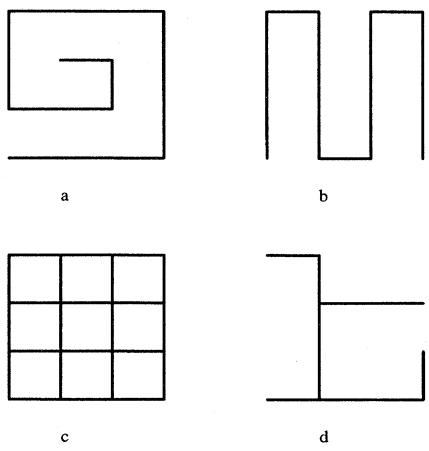

FIG. 1. Possible ground states of the infinite branched polymer in (a), (b) the contact-rich region of the compact phase, (c) the bond-rich region of the compact phase, and (d) the extended phase.

*Permanent address.

fined in the literature [9,11] in terms of two sets of variables and it is useful to give both of them here.

$$\mathcal{Z}=\sum_n x^n \mathcal{Z}_n(y,\tau)=\sum_{n,b,k} a_{n,b,k} x^n y^b \tau^k$$

$$=\sum_n e^{\beta_0 n}\mathcal{Z}_n(\beta_1,\beta_2)=\sum_{n,s,k} a_{n,s,k}\exp(\beta_0 n+\beta_1 s+\beta_2 k), \tag{1.1}$$

where $a_{n,b,k}$ stands for the number of graphs with given n,b,k, and x,y,τ and β_0,β_1,β_2 are fugacities. The relationship between the two sets of variables is given by

$$x=\exp(\beta_0+\gamma\beta_1), \quad y=\exp(-2\beta_1), \quad \tau=\exp(\beta_2-2\beta_1). \tag{1.2}$$

The infinite lattice animal can be described either by taking $n\to\infty$ or by fixing one of the three fugacities in terms of the other two [2], say $x=x_c(y,\tau)$ or $\beta_0=\beta_{0c}(\beta_1,\beta_2)$ (see also below).

The compact and extended phases can be distinguished from the scaling behavior of the mean radius of gyration, $\langle R_N\rangle$, with the number of monomers N, viz.,

$$\langle R_N\rangle\sim N^{\nu}. \tag{1.3}$$

The phase diagram is sketched in Fig. 2. First, there is a (second-order) transition from an extended state (with $\nu\simeq 0.6408$ in two dimensions [32]) where the different branches of the lattice animal are widely separated, to a compact state ($\nu=1/d$). The locations of this extended-compact transition which follow either from exact enumeration [9,33] or transfer matrix calculations [32,11] are in good agreement with each other. However, there is an important discrepancy, which is the subject of this paper. While the enumeration studies [9,33] suggest the existence of an *additional* transition between two distinct compact phases, no sign of such a transition was found using the transfer matrix [11].

The reason a compact-compact transition could in principle be present can be better understood by looking at Fig. 1. Among the compact configurations [(a), (b), (c)] which can fill all space, there are two different types. The first is a contact-rich (and almost linear) branched polymer [Figs. 1(a) and 1(b)] and the second type is a cycle-rich branched polymer [Fig. 1(c)]. Contact-rich configurations are expected to provide the dominant contributions to $\mathcal{Z}$ in the $\tau\to\infty$ region, whereas cycle-rich configurations are expected to dominate as $y\to\infty$. The question is whether or not there exists a sharp transition between the compact configurations. (A similar kind of transition has recently been discussed in the polymer literature [12,34] and it displays some analogies with phenomena occurring in polymer gels, for which a multiplicity of phases can be realized in the collapse process [35].)

Our aim in this paper is to further investigate the existence or otherwise of this transition, by considering some approximations which render the model analytically solvable. This will be done using an exact mapping onto an extended q-state Potts model, which will be defined in the next section. The results of the approximate analysis of the extended q-state Potts model will then be reinterpreted in terms of the lattice animal. Some of these results were already

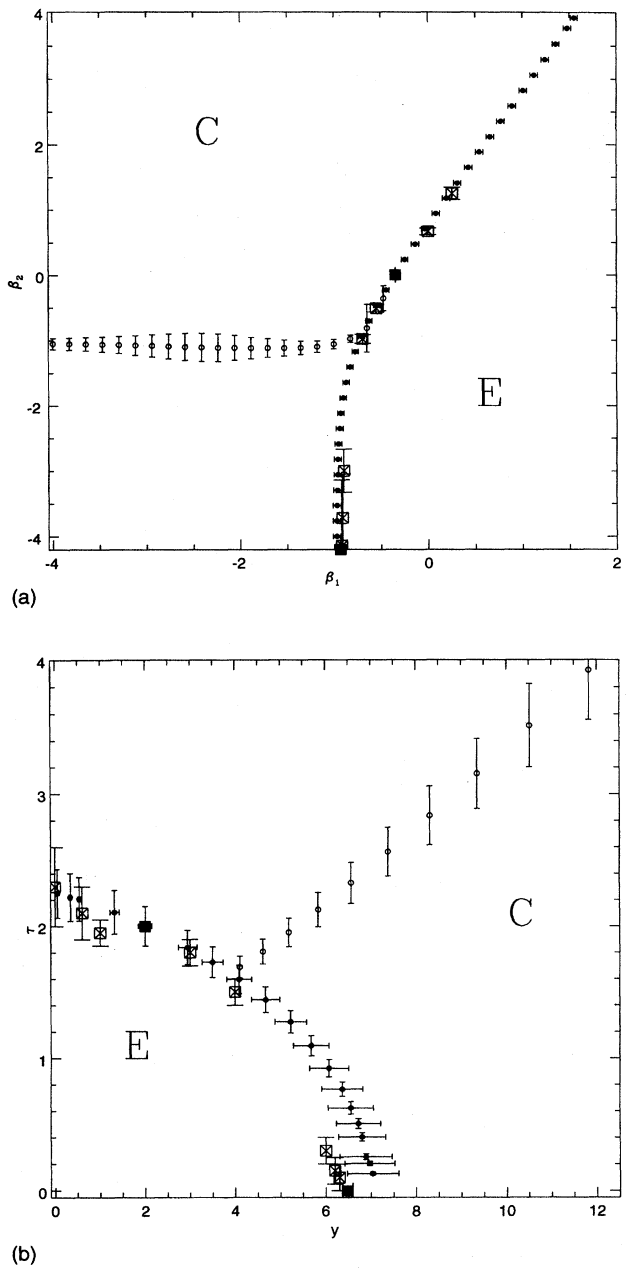

FIG. 2. Numerical phase diagram of the infinite branched polymer in two dimensions in the variables (a) $\beta_1-\beta_2$, (b) $y-\tau$ which are defined in the text. The extended phase is indicated by E and the compact phase by C. Results are from cluster enumeration (circles) [9,33] and the transfer matrix (open squares) [11]. The full circles give the extended-compact collapse transition while the open circles give the compact-compact transition predicted in [9,33]. The black squares give the exactly known transition at the percolation point [9,11] and the collapse transition in the strong-embedding limit [31].

stated without derivation in [36]. In Sec. III we present the exact solution of the extended Potts model on the Bethe lattice and derive the phase diagram. This calculation will be supplemented in Sec. IV by an analysis of the fixed-point structure of the model resulting from the Migdal-Kadanoff

renormalization group equations. In both schemes our results support a phase diagram with a single extended and a single compact phase. These are separated by a line of θ transitions, divided into two sections which fall into different universality classes and which are separated by a higher-order multicritical point, which coincides with critical percolation. In Sec. V we illustrate further the role of the competition of the contact-rich and cycle-rich states by studying two-dimensional *directed* branched polymers, where the cycles are absent. We find a single line of θ transitions in the directed percolation universality class. Finally, in Sec. VI we present our conclusions.

II. EXTENDED POTTS MODEL FORMULATION

We are interested in the phase diagram of infinite branched polymers which are defined by the generating function $\mathscr{Z}$ in Eq. (1.1). Two existing results can serve as a guide. First, in the case of *strong embedding* (no contacts allowed), the extended-compact transition is at $y \simeq 6.48$ and $\tau = 0$ [31]. Secondly, it was shown [9,11] that along a certain line in the x,y,τ (or β_0,β_1,β_2) space the branched polymer can be mapped onto percolation. The percolation critical point corresponds to the following point on the θ transition line:

$$y_p = 2, \quad \tau_p = 2 \tag{2.1}$$

(or $\beta_1 = -\frac{1}{2}\ln 2$, $\beta_2 = 0$).

Our approach is based on the known [24,37,26,25] exact relation of the lattice animal with the extended q-state Potts model with the classical Hamiltonian

$$\mathscr{H} = -J\sum_{(i,j)} \delta_{\sigma_i,\sigma_j} - L\sum_{(i,j)} \delta_{\sigma_i,1}\delta_{\sigma_j,1} - H\sum_i \delta_{\sigma_i,1}, \tag{2.2}$$

where $\sigma_i = 1,2,\ldots,q$ and the fugacities are expressed in terms of J,L,H as

$$x = \exp[-H-\gamma(J+L)], \quad y = (e^J-1)e^{J+L}, \quad \tau = e^{J+L}. \tag{2.3}$$

The relation of this extended Potts model with the lattice animal problem is

$$\mathscr{Z} = f_{\text{Potts}} = \lim_{q\to 1}\frac{\partial}{\partial q}\ln\tilde{Z}, \quad \tilde{Z} = \sum_{\{\sigma\}} e^{-\mathscr{H}}, \tag{2.4}$$

where f_{Potts} is the Potts model free energy. The connection in Eq. (2.4) can be established by considering the graphs in the high-temperature expansion of the Hamiltonian (2.2) and matching the weights in such a way as to reproduce the branched polymer generating function. Thus calculating the phase diagram of the Potts model gives information about the phases of the animal problem. *This correspondence is exact.* However, approximations are needed to treat the extended Potts model. Having solved the extended Potts model in the approximations stated below, we shall reinterpret the results for the extended Potts model phase diagram in terms of the lattice animal collapse transition(s). We shall pursue two approaches.

(1) The exact solution on the Bethe lattice should give the correct topology of the phase diagram for sufficiently large spatial dimensions d. While the Bethe lattice solution is expected to become exact in the $d\to\infty$ limit and should have the same universality properties as a mean-field treatment (see [38] for a detailed discussion), it has the advantage over mean-field theories that the self-consistency equations to be dealt with are considerably simpler. We point out that for the original branched polymer problem, a Bethe lattice solution is of little interest, since contact interactions are eliminated on the Bethe lattice by construction. Contact interactions may be kept by considering the lattice animal on a cactus lattice, which is the dual lattice of the Bethe lattice, see [39]. On the other hand, contact interactions are not projected out by our treatment of the Bethe lattice approximation in the extended Potts model, as we shall see below.

(2) We supplement this by an analysis of the fixed-point structure of the model, using the Migdal-Kadanoff approximation, which should become reliable in $d = 1+\epsilon$ dimensions, as reviewed in [40]. Our finding that the structure of the phase diagram is the same in *both* approximations makes it plausible that the topology is valid for all dimensions. This result is the more remarkable since it is known, for example in three-component lattice gases [41], that the phase diagrams found from mean-field theory and Migdal-Kadanoff approximations may in general be distinct.

Our aim is to find the phase diagram of *infinite* lattice animals through a study of the equivalent extended Potts model. It is well known that taking the limit $n\to\infty$ corresponds to finding critical points of the Hamiltonian (2.2). Transitions between different infinite polymer states then correspond to multicritical points within the critical manifold of the extended Potts model, see [2].

We now recall a relationship [11] which will later be used to simplify the calculations on the Bethe lattice. In principle, we are interested in the lattice animal free energy F. In the canonical ensemble (with n fixed), it is rigorously known [9,13] that

$$F(\beta_1,\beta_2) = \lim_{n\to\infty} n^{-1}\ln\mathscr{Z}_n(\beta_1,\beta_2) \tag{2.5}$$

exists and is a convex function in β_1 and β_2. We now apply Eq. (2.5) to fix x in the grand canonical ensemble such that we describe the infinite lattice animal. Using Eq. (2.5), the animal generating function takes the asymptotic form $\mathscr{Z} \sim \Sigma_n (xe^F)^n$, which diverges at the critical point x_c given by

$$F = -\ln x_c. \tag{2.6}$$

Thus, working in the grand canonical ensemble, it is sufficient to find x_c as a function $x_c(y,\tau)$ of the other fugacities y and τ. Once the critical value of x is obtained as a function $x_c(y,\tau)$, the canonical free energy follows from Eq. (2.6).

III. BETHE LATTICE SOLUTION

We now describe in detail the exact solution of the $q\to 1$ extended Potts model on the Bethe lattice.

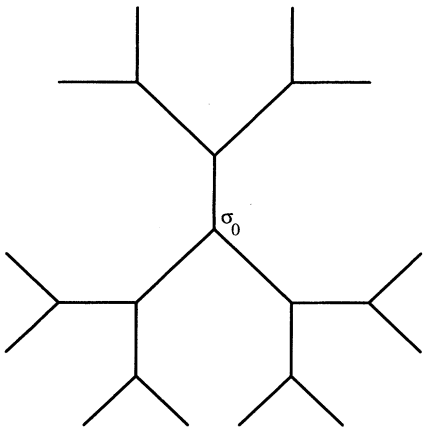

FIG. 3. Bethe lattice with coordination number $\gamma=3$ and central spin σ_0.

A. Generalities

Consider a Cayley tree (Fig. 3) with $\gamma=3$ nearest neighbors for each site. Following the terminology of [38], by Bethe lattice solution we mean the behavior deep inside the Cayley tree. Let σ_0 denote the central spin of the Bethe lattice. Then the extended Potts model partition function is

$$\tilde{Z}=\sum_{\sigma_0} e^{H\delta_{\sigma_0,1}} \sum_{\{s\}} \prod_{j=1}^{3} Q_n(\sigma_0|s^{(j)}), \tag{3.1}$$

where $s^{(j)}$ denotes the spins in the jth sub-branch and

$$\begin{aligned} Q_n(\sigma_0|s)=&\exp(J\delta_{\sigma_0,s_1}+L\delta_{\sigma_0,1}\delta_{s_1,1}+H\delta_{\sigma_0,1}) \\ &\times\exp\Bigg(J\sum_{(i,j)}{}' \delta_{s_i,s_j}+L\sum_{(i,j)}{}' \delta_{s_i,1}\delta_{s_j,1} \\ &+H\sum_{i}{}' \delta_{s_i,1}\Bigg), \end{aligned} \tag{3.2}$$

where Σ' is a sum over one sub-branch of which the first site is s_1.

B. Derivation of the self-consistency equations

We define, following Baxter [38],

$$g_n(\sigma_0)=\sum_{\{s\}}{}' Q_n(\sigma_0|s), \tag{3.3}$$

where n refers to the number of iterations performed in the construction of the Cayley tree. Recursion relations for the g_n are

$$\begin{aligned} g_n(\sigma_0)=&\sum_{s_1=1}^{q} \exp(J\delta_{\sigma_0,s_1}+L\delta_{\sigma_0,1}\delta_{s_1,1} \\ &+H\delta_{s_1,1})[g_{n-1}(s_1)]^2. \end{aligned} \tag{3.4}$$

Having solved Eqs. (3.4) and thus obtained the g_n, the thermodynamics is determined completely.

The analysis of Eqs. (3.4) can be simplified, in analogy to the procedure described in [42], by introducing the variables

$$\Xi_n=\frac{g_n(\sigma_0\neq 1,2,3)}{g_n(1)}, \quad \Upsilon_n=\frac{g_n(2)}{g_n(1)}, \quad Z_n=\frac{g_n(3)}{g_n(1)}, \tag{3.5}$$

which, as will become apparent later, are sufficient to describe the full thermodynamics. Our choice of variables was motivated by the mean-field treatment of the ordinary q-state Potts model in an external symmetry-breaking field [42]. There it was shown that for the distinct ground states corresponding to different phases the order parameter either has the same value for all its q components or that at most the order parameter component which is directly coupled to the field may be different from the others. In (3.5) we generalize that result in order to allow for the possibility of a compact-compact transition besides the expected θ transition. As $n\to\infty$, the variables in (3.5) tend to fixed-point values Ξ,Υ,Z, which can be determined from the recursion relations (3.4). At this stage, we take the $q\to 1$ limit [see (2.4)] and find the self-consistency relations

$$\begin{aligned} \Xi&=\frac{x^{-1}\tau^{-3}+\Upsilon^2+Z^2+(y/\tau-2)\Xi^2}{x^{-1}\tau^{-2}+\Upsilon^2+Z^2-2\Xi^2}, \\ \Upsilon&=\frac{x^{-1}\tau^{-3}+(y/\tau+1)\Upsilon^2+Z^2-2\Xi^2}{x^{-1}\tau^{-2}+\Upsilon^2+Z^2-2\Xi^2}, \\ Z&=\frac{x^{-1}\tau^{-3}+\Upsilon^2+(y/\tau+1)Z^2-2\Xi^2}{x^{-1}\tau^{-2}+\Upsilon^2+Z^2-2\Xi^2}. \end{aligned} \tag{3.6}$$

Equations (3.6) can be decoupled after some transformations of the variables. We then find that there are four cases which must be considered separately. As we now show, in each case the problem of solving a set of three coupled equations can be reduced to the solution of a single quartic equation.

(1) Case A: $\Xi=\Upsilon=Z$. The fixed-point equation is a quadratic equation in Ξ, with the solutions

$$\Xi_{\pm}=\frac{1\pm\sqrt{1-4xy}}{2xy\tau}. \tag{3.7}$$

From Eq. (3.6), it is clear that Ξ_- is the stable solution which, using Eq. (2.4), determines the lattice animal generating function

$$\mathscr{Z}=x\tau^3\Xi_-^3. \tag{3.8}$$

These solutions are real provided $4xy\leq 1$. Criticality corresponding to an infinite lattice animal is recovered at

$$x_c=\frac{1}{4y}. \tag{3.9}$$

(2) Case B: $\Xi=Z\neq\Upsilon$. We introduce the variables

$$u=\Xi+\Upsilon, \quad v=\Upsilon-\Xi. \tag{3.10}$$

For $v=0$, case A is recovered. For $v\neq 0$, a factor v cancels from the fixed-point equations (3.6) giving

$$v=\frac{y}{\tau}-\frac{1}{x\tau^2}\frac{1}{u}, \tag{3.11}$$

$$x^2y\tau^4(u^4-4u^3)+x\tau^2[4(\tau-1)-xy^3]u^2+2xy^2\tau u-y=0. \tag{3.12}$$

Case C: $\Xi\neq\Upsilon=Z$. We introduce again u and v defined by (3.10). For $v=0$, case A is again recovered. For $v\neq 0$, a factor v cancels giving

$$v=\frac{y}{2\tau}-\frac{1}{2x\tau^2}\frac{1}{u}, \tag{3.13}$$

$$x^2y\tau^4(u^4-4u^3)+x\tau^2\left(4(\tau-1)-\frac{1}{4}xy^3\right)u^2 + \frac{1}{2}xy^2\tau u-\frac{y}{4}=0. \tag{3.14}$$

Case D: $\Xi\neq\Upsilon\neq Z$. We define new variables

$$a=\Upsilon+Z,\quad b=\Upsilon-Z \tag{3.15}$$

and rewrite the fixed-point equations (3.6) in terms of Ξ,a,b. $b=0$ corresponds to case C. For $b\neq 0$, a factor b cancels giving

$$b^2=-a^2+4\Xi^2+\frac{2y}{\tau}a-\frac{2}{x\tau^2} \tag{3.16}$$

together with

$$\frac{y}{\tau}a^2=\frac{2}{x\tau^3}-4\Xi^2+\left(\frac{y}{\tau}+2\right)\left(\frac{y}{\tau}a+2\Xi^2-\frac{1}{x\tau^2}\right),$$
$$\frac{y}{\tau}a\Xi=\frac{1}{x\tau^3}+\frac{y}{\tau}\Xi^2+\frac{y}{\tau}a-\frac{1}{x\tau^2}. \tag{3.17}$$

Provided $\Xi\neq 1$, we solve the second of Eqs. (3.17) for a,

$$\frac{y}{\tau}(\Xi-1)a=\frac{y}{\tau}\Xi^2+\frac{1-\tau}{x\tau^3}, \tag{3.18}$$

and find

$$x^2y^2\tau^4[\Xi^4+(y/\tau-2)\Xi^3]-xy^2\tau^2(1+xy\tau^3)\Xi^2 + xy\tau[y(1+\tau)+2\tau(1-\tau)]\Xi-(1-\tau)^2-xy^2\tau=0. \tag{3.19}$$

Note that the relation between Ξ and Z remains unspecified.

C. Analysis of the self-consistency equations

The problem has been reduced to the solution of three quartic equations (3.12), (3.14), and (3.19). Further analysis is greatly simplified by numerically checking that all solutions in case D where Ξ, Υ, and Z are *a priori* different, reduce to one of case B, with $\Xi=Z$. As we shall show below, this implies that there are only two distinct phases for the infinite lattice animal on the Bethe lattice. In particular, that means if any two branches of the lattice animal generating function calculated in cases A, B, and C meet, all three solutions have to coincide. It follows that the topology of the phase diagram calculated in the whole (Ξ,Υ,Z) space is the same as would have been found when only considering (Ξ,Υ) space, with $\Upsilon=Z$. We expect the same reduction to occur in even more generic setups than done in Eq. (3.5).

We only have to consider cases A, B, and C. We introduce a new variable

$$p=u\tau,\quad u=\Xi+\Upsilon. \tag{3.20}$$

We recall from (2.6) that in order to get the infinite lattice animal free energy in the canonical ensemble, it is enough to know x as a function of y and τ. Solving for $x=x_c(p;y,\tau)$ rather than solving for p (or u) has the further advantage of going from quartic to quadratic equations. p now plays the role of an order parameter and will be fixed by maximizing $x(p)$ with respect to p. We find

(1) Case A. We have

$$A(p;y,\tau):=x^{(A)}(p;y,\tau)=\frac{2(p-2)}{yp^2}. \tag{3.21}$$

(2) Case B. The equation is

$$x^2(yp^4-4y\tau p^3)+x[4(\tau-1)p^2-xy^3p^2+2y^2p]-y=0, \tag{3.22}$$

with the solutions

$$B_\pm(p;y,\tau):=x_\pm^{(B)}(p;y,\tau) =\frac{2(1-\tau)p-y^2}{py(p^2-4\tau p-y^2)} \pm\frac{\sqrt{p(4\tau^2-8\tau+4+y^2)-4y^2}}{\sqrt{p}(p^2-4\tau p-y^2)y}. \tag{3.23}$$

(3) Case C. The equation is

$$x^2(yp^4-4y\tau p^3)+x\left(4(\tau-1)p^2-\frac{1}{4}xy^3p^2+\frac{1}{2}y^2q\right) -\frac{y}{4}=0, \tag{3.24}$$

with the solutions

$$C_\pm(p;y,\tau):=x_\pm^{(C)}(p;y,\tau)=\frac{1}{2}B_\pm(p;y/2/\tau). \tag{3.25}$$

To get the equilibrium physics, we have to minimize the lattice animal free energy $F(y,\tau)$ [see Eqs. (2.5) and (2.6)] with respect to p or equivalently to maximize $x(p;y,\tau)$. For case A, we have

$$F=-\ln x=-\ln\left(\frac{2(p-2)}{p^2y}\right),\quad \frac{\partial F}{\partial p}=\frac{p-4}{p(p-2)},$$
$$\left.\frac{\partial^2F}{\partial p^2}\right|_{p=4}=\frac{1}{8}>0, \tag{3.26}$$

and F has a single minimum at $p=4$. Indeed, $F=\ln(4y)$ evaluated at $p=4$ is concave in y.

It remains to be seen under which conditions this local minimum of $F^{(A)}$ is the absolute minimum of F. (It is

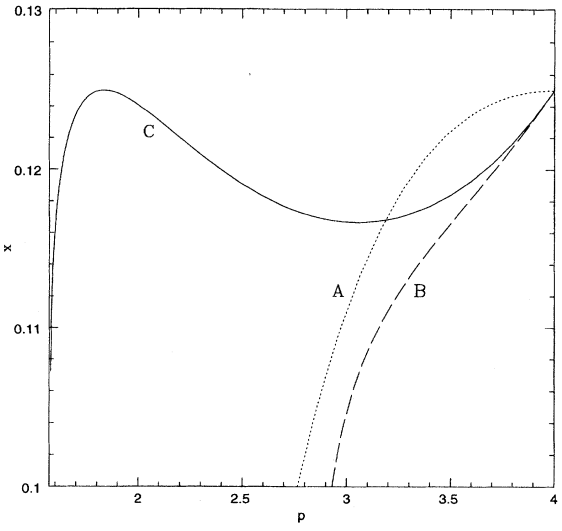

FIG. 4. p dependence of the three solutions A (dotted), B_- (dashed), and C_- (full) of the Bethe lattice recursion relations, for $y=2, \tau=1.619\,49$.

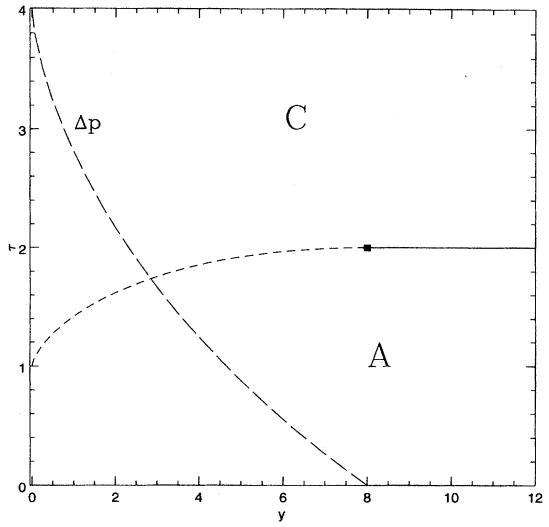

FIG. 5. Phase diagram of the extended Potts model on the Bethe lattice. The phase labeled A corresponds to the extended lattice animal while C corresponds to the compact lattice animal. The line indicated by short dashes is first order and the full line is second order. The black square at $y=8, \tau=2$ indicates their meeting point. The jump Δp as a function of y between the phases A and C along the first-order line is indicated by the long-dashed line and is shown on the same scale.

enough to consider B_- and C_-, since the other two solutions B_+, C_+ have no maxima with respect to p.) From the above it is clear that if any two of the solutions A, B, and C meet, we have in fact a simultaneous meeting of all three of them. This common meeting point occurs at $p=4$,

$$A(4;y,\tau)=B_-(4;y,\tau)=C_-(4;y,\tau)=\frac{1}{4y}, \quad \tau\geq 1,$$

$$A(4;y,\tau)=B_+(4;y,\tau)=C_+(4;y,\tau)=\frac{1}{4y}, \quad \tau\leq 1 \tag{3.27}$$

(see Fig. 4). In addition, we have checked that

$$C_-(p;y,\tau)\geq B_-(p;y,\tau). \tag{3.28}$$

For an example illustrating the solutions A, B_-, C_-, see Fig. 5. This implies that there are just two distinct phases of the lattice animal which are described by the two solutions $A(p;y,\tau)$ and $C_-(p;y,\tau)$. Furthermore, we want solutions such that the fugacity x is real and positive. This yields the condition

$$p\geq\begin{cases} 2, & \text{case A} \\ \dfrac{(y/2)^2}{(\tau-1)^2+(y/4)^2}, & \text{case C.} \end{cases} \tag{3.29}$$

On the other hand, the unstable solution Ξ_+ from case A always corresponds to $p\geq 4$. Furthermore, we argue in the Appendix that for $p>4$ the solution C_- is not a stable solution of the self-consistency relations (3.6). We therefore must have

$$p\leq 4. \tag{3.30}$$

To get the transition lines between the two phases, note that $\partial C_-/\partial p=0$ if and only if $\tau=2$. Furthermore

$$C_-(p;y,2) \text{ has at } p=4 \text{ a } \begin{cases} \text{maximum if } y>8 \\ \text{turning point if } y=8 \\ \text{minimum if } y<8. \end{cases} \tag{3.31}$$

To locate the transitions, one must distinguish two cases. First, for $y<8$, one has a first-order transition. It is given by the conditions

$$C_-(p;y,\tau)=A(4;y,\tau)=\frac{1}{4y},$$

$$\frac{\partial C_-}{\partial p}(p;y,\tau)=0, \tag{3.32}$$

$$\frac{\partial^2 C_-}{\partial p^2}\leq 0.$$

At this transition point, p jumps from its value $p=4$ for τ small to a new value $p_c(y,\tau)<4$. The location of the line and p_c have to be found numerically.

Second, for $y>8$ and $\tau>2$, numerical studies show that $C_-(p;y,\tau)$ has a maximum at some value $p'<4$. For all $p<4$, $C_->A$ and the state described by p' is the equilibrium ground state. As $p\to 4$, the two solutions approach each other continuously.

Finally, for $y=8$ and $\tau=2$, the second-order line ends in a tricritical point. The two transitions are shown in Fig. 6. We also show the jump in p, $\Delta p=4-p_c(y,\tau)$, and observe that $\Delta p\sim(8-y)$ for $y\to 8^-$.

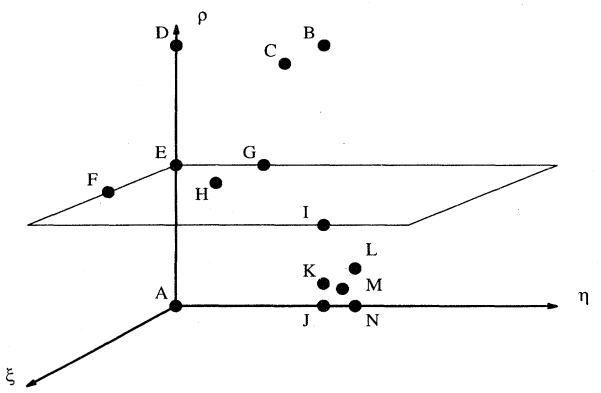

FIG. 6. Fixed-point structure which follows from the Migdal-Kadanoff renormalization group for the extended Potts model (2.2) for $q \to 1$ and $\epsilon \to 0$. The plane $\rho = 1$ is also shown to guide the eye.

D. Summary

Studying the phase diagram of the extended Potts model in the $q \to 1$ limit on the Bethe lattice, we find that there are two distinct phases (A and C above) on the manifold corresponding to the infinite lattice animal. The transition between them is first order for $y < 8$ and second order for $y > 8$. There is a tricritical point at $y = 8$, $\tau = 2$. The Bethe lattice calculation corresponds to a mean-field calculation [38]. Detailed comparison [38] of the exact solution of the simple q-state Potts model (that is, $L = H = 0$) in two dimensions with the Bethe lattice solution suggests that the latter faithfully represents the model behavior for infinite dimensionality. We expect the same for the more general models treated here.

IV. MIGDAL-KADANOFF RENORMALIZATION GROUP

In the preceding section, we studied the extended Potts model (2.2) using an approximation which should become more reliable with increasing dimensionality. We now wish to complement this calculation by a Migdal-Kadanoff renormalization group study. The Migdal-Kadanoff approximation preserves the self-duality property of several two-dimensional models (in particular the q-state Potts model, see [40,43]) and thus yields the phase diagram exactly. The bond-moving approximation involved is exact at zero temperature and its predictions for exponents are exact to order ϵ in $d = 1 + \epsilon$ dimensions, as reviewed in detail in [40]. We therefore hope that the renormalization group calculation will provide reliable information on the fixed-point structure for low dimensions.

The Hamiltonian (2.2) has already been investigated using a Migdal-Kadanoff renormalization group by Coniglio [26]. He used a rescaling factor $b = 2$ in dimensionality $d = 2$ and considered $q = 1$, rather than $q \to 1^+$. He identified four nontrivial fixed points which correspond to (1) an extended lattice animal phase, (2) a compact phase, (3) a percolation point, and (4) a tricritical point analogous to a θ point. These are not sufficient to describe the topology of Fig. 2 and therefore it seemed useful to look again at the calculation with particular emphasis on the possibility of the occurrence of a compact-compact transition.

Here, we shall consider the case $d = 1 + \epsilon$. Furthermore, as will become apparent, the limit $q \to 1$ has to be taken with care, because the fixed-point structure changes at $q = 1$. For $d = 1 + \epsilon$ and $b = 2$ the Migdal-Kadanoff recursion equations for the extended Potts Hamiltonian (2.2) are

$$\xi' = \left(\frac{\xi[1 + \rho + (q-2)\eta]}{1 + \xi^2 + (q-2)\eta^2} \right)^{b^\epsilon}, \tag{4.1}$$

$$\eta' = \left(\frac{\xi^2 + 2\eta + (q-3)\eta^2}{1 + \xi^2 + (q-2)\eta^2} \right)^{b^\epsilon}, \tag{4.2}$$

$$\rho' = \left(\frac{\rho^2 + (q-1)\xi^2}{1 + \xi^2 + (q-2)\eta^2} \right)^{b^\epsilon}, \tag{4.3}$$

where

$$\xi = \exp(H/2 - J), \quad \eta = \exp(-J), \quad \rho = \exp(L + H). \tag{4.4}$$

Equations (4.1)–(4.3) were obtained by performing a one-dimensional decimation followed by bond moving [40,41].

The fixed-point structure that follows from the recursion equations (4.1)–(4.3) is complicated and q dependent. However, using the $q = 2,3$ cases as a guide [41], in the two limits of interest to us ($q \to 1$ and $\epsilon \to 0$) a clear pattern appears and 14 fixed points can be identified. These are listed in Table I, together with the eigenvalues of the Jacobian evaluated at the fixed points. We also illustrate the fixed-point structure in Fig. 6.

Note that the fixed points naturally divide into three groups. The first group contains the fixed points B, C, and D for which $\rho^* = \infty$. The second group, which is the one we shall be interested in, contains the fixed points, E, F, G, H, and I which all have $\rho^* \simeq 1$. Finally, the third group contains the fixed points with $\rho^* \approx 0$, namely A and the cluster of fixed points around $y \simeq 1$, J, K, L, M, and N. For $q \to 1$, the last five points merge to a single fixed point.

To understand the physics, we begin by singling out the completely attractive (or trivial) fixed points. Reading from Table I the fixed points B, C, D and A, J, N only have eigenvalues which are smaller than one. Hence they cannot describe the critical behavior of the infinite branched polymer. Next, we consider the cluster of five fixed points near to $(\xi^*, \eta^*, \rho^*) \approx (0,1,0)$. One ($M$) has two relevant eigenvalues, while two (K and L) have one relevant eigenvalue, with an associated exponent $y = d$. From the eigenvectors, we have checked that the renormalization group flow from the vicinity of one of the fixed points M, K, L always goes towards the trivial stable fixed points J and N. Since these five fixed points are going to merge into a single fixed point in the $q \to 1$ limit and none of them has three relevant eigenvalues as would be required from a percolation fixed point, we conclude that they cannot govern any part of the phase diagram of the branched polymer problem. We thus find that the fixed-point structure depends on carefully taking the $q \to 1^+$ limit, rather than simply setting $q = 1$.

It remains to consider those fixed points which are close to the $\rho^* = 1$ plane. Two of these (E and I) are independent of both q and ϵ and have one relevant eigenvalue. For the fixed point E, the relevant direction is characterized by the exponent $1/\nu = d = 1 + \epsilon$. This is characteristic of a compact

TABLE I. Fixed points of the Migdal-Kadanoff recursion relations. The following abbreviations are used: $\alpha=\frac{1}{2}\exp(-1/\epsilon)$, $\beta=\exp(-1/[\epsilon 2\ln 2])$, $\gamma=1/(2-q)+[\ln(2-q)/(q-2)](e-1)$, $\delta=(q-1)/(q-2)+[(e-1)/(q-2)]\{(q-1)\ln[(q-2)/(q-1)]-2\ln(2-q)\}$, $e=2^{\epsilon}$, $\lambda_1=\{(q-2)[\ln(2-q)]/(q-1)\}(2^d-2)$, $\lambda_2=[2(q-2)/(q-1)](e-1)\ln(2-q)$. Analytic expressions are correct to leading order in ϵ or to the given order in $e-1$. The numerical eigenvalues for the fixed points F, G, and H are correct up to terms $O(q-1)^2$.

	ξ	η	ρ	Eigenvalues			Comments
A	0	0	0	0	0	0	
B	0	1	∞	0	0	0	
C	∞	1	∞	0	0	0	
D	0	0	∞	0	0	0	
E	0	0	1	0	0	2^d	
F	β	0	1	0.738	1.23	2.014	$\epsilon=0.01$
				0.736	1.213	2	$\epsilon\to 0$
G	0	β	1	0	1.22	2.014	$\epsilon=0.01$
				0	1.213	2	$\epsilon\to 0$
H	α	α	1	1.0045	1.0045	2.014	$\epsilon=0.01$
				1+	1+	2	$\epsilon\to 0$
I	1	1	1	0	0	2^{d-1}	
J	0	1	0	0	0	0	
K	0	1	$(q-1)^{e/(2e-1)}$	0	0	2^d	
L	0	γ	δ	0	λ_1	2^d	
M	1.19×10^{-8}	1	0.010	0	1.97	2.002	$q=1.01, e=1.001$
N	0	γ	0	0	0	λ_2	

object and we therefore conclude that this fixed point controls the compact phase of the infinite branched polymer. For the fixed point I, the single relevant eigenvalue is $1/\nu=d-1$. Since $\nu>1/d$, we expect this to describe a noncompact phase and the fixed point I to govern the extended phase of the polymer.

The fixed points F, G, and H are dependent on q and ϵ, but for $q<2$ all appear in the plane $\rho=1$, to leading order in ϵ. As d decreases they move towards the point E. The fixed point H has three relevant eigenvalues and therefore represents the percolation fixed point [which is realized for $H=0$ and $L=0$ in (2.2) and for $d=2$ the Migdal-Kadanoff approach is known [40,43] to correctly reproduce the exact critical point]. F and G are tricritical points and govern the renormalization group flow along the two critical lines leaving the percolation point H. We point out that the fixed point G is only found when the limit $q\to 1^+$ is carefully taken. However, if one simply sets $q=1$, that fixed point is missed, in agreement with the earlier work of Coniglio [26].

Thus we predict a line of θ points which contains two segments falling into two distinct universality classes and meeting at the percolation point. The θ line separates the extended phase from a single compact phase.

V. DIRECTED LATTICE ANIMALS

So far, in this paper we have considered the structure of the phase diagram of the infinite branched polymer. Although the interplay of the different ground state (see Fig. 1) in the contact-rich and contact-poor regions of the compact phase might at first sight suggest the existence of a compact-compact transition, this was not supported by our (albeit approximate) calculations. To provide some insight into the role of the different ground states, we now wish to consider a model where the spiraling or folding ground states shown in Figs. 1(a) and 1(b) are eliminated.

For this reason, we now consider *directed* branched polymers. This model is defined in complete analogy with the system discussed so far, but requiring that the bonds, solvents, and contacts are directed. We use a square lattice with the preferred direction along a lattice diagonal. Animal configurations are allowed only if (1) they start from a single site, (2) all bonds have a component in a preferred direction, and (3) the solvents and contacts counted in the generating function have a component in the preferred direction. The special case where contacts are forbidden (that is, the limit $\beta_2\to-\infty$) was studied previously by Dhar [44].

The interest in this model arises because due to the directedness condition ground states of the *undirected* lattice animals in the contact-rich region ($\beta_1\to-\infty,\beta_2\to\infty$) are not allowed. Indeed, the phase diagram of the directed model (Fig. 7) is quite different, as we shall now show.

For directed lattice animals, it is always possible to reduce the problem to the "strong-embedding" ($\beta_2\to-\infty$) case. To see this, consider a strongly embedded lattice animal (where all neighboring sites are connected by bonds). Strong embedding is broken when some of the bonds are replaced by contacts. We now ask how often these replacements of bonds by contacts can be made.

Because of the directedness, it is clear that bonds can be replaced by contacts only if the strongly embedded lattice animal contains closed loops. Furthermore, each loop contains exactly one "final" site. Only one of the two bonds leading to this final site may be replaced by a contact because of condition (1). Now, consider a directed lattice animal with c loops and denote by $g(c,k)$ the number of ways

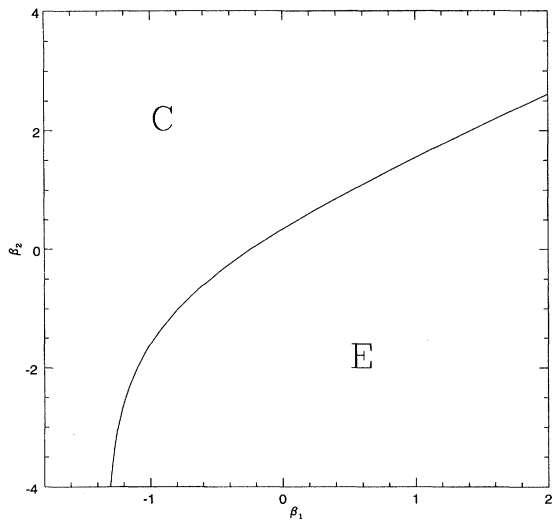

FIG. 7. Phase diagram for the directed branched polymer. The extended phase is indicated by E and the compact phase by C.

of replacing exactly k of the bonds by contacts. Obviously, $g(c,k)=0$ if $k>c$, since no loop can be cut twice. It is also clear by inspection that $g(c,0)=1$ and $g(c,1)=2c$. Also, for $k\geq 2$ the recursion formula

$$g(c,k)=2g(c-1,k-1)+g(c-1,k) \tag{5.1}$$

is valid. To see this, imagine placing the first contact onto the directed lattice animal. Single out one of the loops. Either this contact cuts this loop, which can be done in exactly two ways, and one then has to place $k-1$ contacts onto an animal with $c-1$ loops or this loop is not cut at all and all k contacts are placed onto the remaining $c-1$ loops. Defining the function

$$f(c;\beta)=\sum_{k=0}^{c} g(c,k)e^{\beta k} \tag{5.2}$$

it is easy using (5.1) to show that for all $c\geq 0$

$$f(c;\beta)=(1+2e^{\beta})f(c-1;\beta)=(1+2e^{\beta})^{c}. \tag{5.3}$$

Consider now the directed lattice animal generating function. On the square lattice, $2n=b+k+s$. Using the Euler relation $c=b-n+1$ and (5.3)

$$\mathcal{Z}=\sum_{\mathcal{G}} a(n,k,s)e^{\beta_0 n}e^{\beta_1 s}e^{\beta_2 k}$$

$$=\sum_{\tilde{\mathcal{G}}}{}' a(n,0,s)e^{\beta_0 n}e^{\beta_1 s}(1+2e^{\beta_2})^{c}, \tag{5.4}$$

where $a(n,k,s)$ is the number of directed lattice animals with n sites, k contacts, and s solvents. $\mathcal{G}$ runs over all directed lattice animals and $\tilde{\mathcal{G}}$ over all strongly embedded directed lattice animals. In the strong-embedded case, $k=0$. Thus $c=n-s+1$ and

$$\mathcal{Z}=(1+2e^{\beta_2})\sum_{\tilde{\mathcal{G}}}{}' a(n,0,s)[e^{\beta_0}(1+2e^{\beta_2})]^{n}\left(\frac{e^{\beta_1}}{1+2e^{\beta_2}}\right)^{s}. \tag{5.5}$$

This is the strongly embedded directed lattice animal, with the effective solvent fugacity

$$e^{\tilde{\beta}_1}=\frac{e^{\beta_1}}{1+2e^{\beta_2}}. \tag{5.6}$$

The strong-embedding model can be mapped onto directed percolation [44]. We have thus shown that the fully directed lattice animal has a single extended-compact transition which is in the directed percolation universality class. (We have also checked that the relationship with directed percolation can be established directly from the fugacities given to the elementary processes of the directed animal model.) In contrast to the undirected model, there is no change of the values of the critical exponents along the transition line.

VI. CONCLUSIONS

In this paper, we have investigated the phase diagram of the extended Potts model (2.2) in the $q\to 1$ limit. We have concentrated on the structure of the manifold of critical points, because this is related to the phase diagram of an infinite branched polymer. Using Bethe lattice and Migdal-Kadanoff renormalization group calculations, we find a line of θ transitions between the extended and the compact phase. The θ line consists of two segments which are controlled by different fixed points. Their meeting point coincides with the percolation critical point. Although these results were obtained from rather drastic approximations, we expect the results coming from these to be reliable for large (Bethe lattice, $d\to\infty$) or small (Migdal-Kadanoff, $d=1+\epsilon$) dimensions, respectively. Furthermore, since the qualitative structure of the phase diagram is the same in both cases, it is plausible that the topology of the phase diagram is indeed independent of the dimensionality. Our results on the structure of the θ line agree with previous numerical calculations using either graph enumeration or transfer matrix techniques.

Our calculations give no evidence for a further transition between two compact phases. While that conclusion does agree with numerical transfer matrix calculations, it is in disagreement with analysis based on graph enumeration. We thus expect the crossing over between the contact-rich ground states in Figs. 1(a) and 1(b) and the bond-rich ground state in Fig. 1(c) to be smooth. While intuitively a phase transition between these ground states might appear plausible at least in two dimensions because a ground state as the one in Fig. 1(a) could be seen as a vortex while the state in Fig. 1(c) is not, the nature of that transition is less apparent in three and higher dimensions. However, graph enumeration predicts [33] a compact-compact transition in three and more dimensions as well.

This does not mean, however, that the different ground states of the model in different regions of the compact phase have no physical role. This is clearly illustrated by the case of *directed* branched polymers, where the spiraling states [Figs. 1(a) and 1(b)] are absent. Then the multicritical point on the θ line found for the *undirected* branched polymer

disappears and the entire θ line is in the directed percolation universality class.

ACKNOWLEDGMENTS

It is a pleasure to thank S. Flesia, A. L. Stella, P. Peard, S. G. Whittington, and J. M. Yeomans for useful discussions. We thank P. Peard for kindly providing his numerical results before publication. M.H. thanks the Dipartimento di Fisica della Università di Padova, where part of this work was done, for hospitality and F.S. thanks the Sub-Department of Theoretical Physics in Oxford where another part was added. M.H. was supported by an EC grant of the "Human Capital and Mobility" program.

APPENDIX

Here we study the stability of the solutions of the self-consistency equations (3.6). These arise from recursions of the form

$$x_{n+1}=f(x_n) \tag{A1}$$

and it is well known that a fixed-point solution $x^*=\lim_{n\to\infty}x_n$ is stable under small perturbations if and only if $|f'(x^*)|<1$. Consider first case A. Then we have the recursion

$$\Xi_{n+1}=f(\Xi_n)=\frac{1}{\tau}+xy\tau\Xi_n^2. \tag{A2}$$

With the solutions $\Xi_\pm$ from Eq. (3.7) we have

$$f'(\Xi_\pm)=1\pm\sqrt{1-4xy} \tag{A3}$$

and thus Ξ_- is the stable and Ξ_+ the unstable fixed point. Since $p_\pm=2\tau\Xi_\pm$, it follows that if $\tau\simeq 2$ as is the case for the A to C transition, we have $p\geq 4$ for the unstable case. Next, we look at case C. We introduce u,v from (3.10) and are interested in the case when v is small, that is, near to the θ transition. Then the following fixed-point equation for u holds:

$$u\simeq\frac{2}{\tau}+\frac{1}{2}xy\tau u^2+O(uv), \tag{A4}$$

which is the same relation as for 2Ξ. From (3.7) it then follows that if $u\geq u_+>1/(xy\tau)$, it is an unstable solution. On the other hand, in the vicinity of the A to C transition we have from (3.9) that at least in the transition region, all solutions which correspond to $p=\tau u>1/(xy)\simeq 4$, will be unstable. They are eliminated by requiring that $p\leq 4$.

[1] P. Flory, *Principles of Polymer Chemistry* (Cornell University Press, Ithaca, 1971).

[2] P. G. de Gennes, *Scaling Concepts in Polymer Physics* (Cornell University Press, Ithaca, 1979).

[3] P. G. de Gennes, J. Phys. (Paris) Lett. **36**, L55 (1975).

[4] V. Privman, J. Phys. A **18**, 3281 (1985).

[5] H. Saleur, J. Stat. Phys. **45**, 419 (1986).

[6] A. Coniglio, N. Jan, I. Maijd, and H. E. Stanley, Phys. Rev. B **35**, 3617 (1987).

[7] F. Seno and A. L. Stella, J. Phys. (Paris) **49**, 739 (1988).

[8] N. Madras, C. E. Soteros, S. G. Whittington, J. L. Martin, M. F. Sykes, S. Flesia, and D. S. Gaunt, J. Phys. A **23**, 5327 (1990).

[9] S. Flesia, D. S. Gaunt, C. E. Soteros, and S. G. Whittington, J. Phys. A **25**, L1169 (1992).

[10] C. Vanderzande, Phys. Rev. Lett. **70**, 3595 (1993).

[11] F. Seno and C. Vanderzande, J. Phys. A **27**, 5813 (1994); **27**, 7937 (1994).

[12] A. L. Stella, Phys. Rev. E **50**, 3259 (1994).

[13] S. Flesia, D. S. Gaunt, C. E. Soteros, and S. G. Whittington, J. Phys. A **27**, 5831 (1994).

[14] M. A. Moore, J. Phys. A **10**, 305 (1977).

[15] M. V. Volkstein, *Molecular Biophysics* (Academic, New York, 1977).

[16] S. P. Obukhov, J. Phys. A **9**, 3655 (1986).

[17] J. L. Cardy, in *Fields, Strings and Critical Phenomena*, Les Houches XLIX, edited by E. Brézin and J. Zinn-Justin (North-Holland, Amsterdam, 1990).

[18] P. Christe and M. Henkel, *Introduction to Conformal Invariance and its Applications to Critical Phenomena* (Springer-Verlag, Heidelberg, 1993).

[19] B. Nienhuis, in *Phase Transitions and Critical Phenomena*, edited by C. Domb and J. L. Lebowitz (Academic, New York, 1987), Vol. 11.

[20] B. Duplantier and H. Saleur, Phys. Rev. Lett. **59**, 539 (1987).

[21] C. Vanderzande, A. L. Stella, and F. Seno, Phys. Rev. Lett. **67**, 2757 (1991).

[22] G. Parisi and N. Sourlas, Phys. Rev. Lett. **46**, 871 (1981).

[23] J. Miller and K. De'Bell, J. Phys. (France) I **3**, 1717 (1993).

[24] M. Giri, M. J. Stephen, and G. S. Grest, Phys. Rev. B **16**, 4971 (1977).

[25] F. Y. Wu, J. Stat. Phys. **18**, 115 (1978); Rev. Mod. Phys. **54**, 235 (1982).

[26] A. Coniglio, J. Phys. A **16**, L187 (1983).

[27] R. Dickman and W. C. Shieve, J. Phys. (Paris) **45**, 1727 (1984).

[28] P. M. Lam, Phys. Rev. B **36**, 6988 (1987).

[29] P. M. Lam, Phys. Rev. B **38**, 2813 (1988).

[30] I. S. Chang and Y. Shapir, Phys. Rev. B **38**, 6736 (1988).

[31] B. Derrida and H. J. Herrmann, J. Phys. (Paris) **44**, 1365 (1983).

[32] B. Derrida and L. De Seze, J. Phys. (Paris) **43**, 475 (1982).

[33] P. Peard, Ph.D. thesis, King's College, London, 1995.

[34] D. Bennett-Wood, J. L. Cardy, S. Flesia, A. J. Guttmann, and A. L. Owczarek, J. Phys. A **28**, 5143 (1995).

[35] A. Annaka and T. Tanaka, Nature (London) **355**, 430 (1982).

[36] M. Henkel, F. Seno, and J. M. Yeomans, Oxford Report No. OUTP-95-56S, 1995 (unpublished).

[37] A. B. Harris and T. C. Lubensky, Phys. Rev. B **24**, 2656 (1981).

[38] R. J. Baxter, *Exactly Solved Models in Statistical Mechanics* (Academic, London, 1982), Chap. 4.

[39] P. D. Gujrati, Phys. Rev. Lett. **74**, 1367 (1995); J. Chem. Phys. **98**, 1613 (1993).

[40] T. W. Burkhardt and J. M. J. van Leeuwen, in *Real Space Renormalization*, edited by T. W. Burkhardt and J. M. J. van Leeuwen (Springer-Verlag, Berlin, 1982), p. 1; T. W. Burkhardt, *ibid.*, p. 33.

[41] M. Kaufman, R. B. Griffiths, J. M. Yeomans, and M. E. Fisher, Phys. Rev. B **23**, 3448 (1981).

[42] A. Baracca, M. Bellesi, R. Livi, R. Rechtman, and S. Ruffo, Phys. Lett. **99A**, 156 (1983).

[43] C. Itzykson and J. -M. Drouffe, *Statistical Field Theory* (Cambridge University Press, Cambridge, England, 1989), Vol. 1, Chap. 4.

[44] D. Dhar, J. Phys. A **20**, L847 (1987).